SURFACE SCIENCE, CLUSTERS, MICELLES, AND INTERFACES

Rate Constants of Surface Reactions in Methanation over Ru/Al_2O_3 Catalyst As Determined by Pulse Surface Reaction Rate Analysis

Toshiaki Mori,*

Government Industrial Research Institute, Nagoya, Hirate-cho, Kita-ku, Nagoya 462, Japan

Akira Miyamoto, Hiroshi Niizuma, Naoki Takahashi, Tadashi Hattori, and Yuichi Murakami

Department of Synthetic Chemistry, Faculty of Engineering, Nagoya University, Furo-cho, Chikusa-ku, Nagoya 464, Japan *(Received: February 18, 1985)*

By use of a new PSRA (pulse surface reaction rate analysis) apparatus equipped with an emissionless infrared diffuse reflectance spectrometer (EDR) and a flame ionization detector (FID), the dynamics of both adsorbed CO and produced CH_4 were simultaneously measured in the CO hydrogenation over Ru/Al_2O_3 catalyst. When a CO pulse was introduced to the catalyst via the H_2 at temperatures above 405 K, an IR absorption band assignable to a linearly adsorbed CO appeared at 2040 cm^{-1}. At the same time an FID response of CH_4 quickly increased. Then the IR absorption of the linear CO gradually decreased with time accompanying the gradual decrease in the FID response of CH_4, indicating that linear CO gradually reacts with H_2 to form CH_4. Since CH_4 is considered to be produced through the hydrogenation of surface carbon species $[(CH_x)_{ad}]$, viz. $(CO)_{ad} \xrightarrow{k_{CO}} (CH_x)_{ad} \xrightarrow{k_{CH_x}} CH_4$, the rate constants of the respective steps (k_{CO} and k_{CH_x}) can be determined from the dynamics of $(CO)_{ad}$ and CH_4 after the CO pulse. It was found that k_{CH_x} is more than 50 times larger than k_{CO}, indicating that on the Ru/Al_2O_3 catalyst the formation of $(CH_x)_{ad}$ from adsorbed CO is much slower than its hydrogenation to CH_4. Furthermore, an H_2–D_2 inverse isotope effect was observed for k_{CO}, suggesting that hydrogen atoms play an important role in the C–O bond dissociation in the CO hydrogenation. A mechanism of the C–O bond dissociation was also discussed on the basis of these results for k_{CO}.

Introduction

A heterogeneous catalytic reaction is composed of various steps including adsorptions, surface reactions, and desorptions. The rate measured by a conventional method is overall one of these processes. The direct determination of rate constants of individual processes is therefore highly desirable for a detailed understanding of the mechanism of the reaction.[1] In principle, measurements of the dynamics of adsorbed species and product molecules can lead to the determination of the rate constants of individual steps involved in the reaction. Several workers have demonstrated the availability of the transient response method for this purpose.[2] We have proposed a pulse surface reaction rate analysis (PSRA) for the same purpose and demonstrated the availability for the dehydration of alcohols on Al_2O_3,[3] cracking of cumene on zeolites,[4] hydrogenolysis of alkylamines on $Co–Mo/Al_2O_3$ catalysts,[5] and methanation on supported Ni and Pd catalysts.[6] In the previous PSRA apparatus, however, only the dynamics of product molecules were measured but that of adsorbed species could not be directly observed.[3-6] This seems to limit further application of the PSRA to various catalyst systems.

The purpose of this study is (i) to develop a new PSRA apparatus which enables us simultaneous measurement of the dynamics of both adsorbed species and product molecule and (ii) to determine rate constants per active sites of surface reactions in the hydrogenation of CO over Ru/Al_2O_3. The new PSRA apparatus has an emissionless infrared diffuse reflectance spectrometer (EDR) and a flame ionization detector (FID); the former serves to measure the dynamics of adsorbed species while the latter measures that of the product molecule. The CO hydrogenation on supported metal catalysts has been found to be composed of several steps including the adsorption of H_2 and CO, dissociation of the adsorbed CO $[(CO)_{ad}]$ to surface carbon $[(CH_x)_{ad}]$ and oxygen $[(OH_y)_{ad}]$ species, and hydrogenation of $(CH_x)_{ad}$ to hydrocarbons with various numbers of carbon atoms.[7] The determination of rate constants of these steps is necessary for a detailed understanding of the reaction mechanism. We have previously found that hydrogen atoms play an important role in the process of the C–O bond dissociation in the CO hydrogenation.[6] The mechanism for this process on Ru/Al_2O_3 is also discussed in terms of the rate constant.

Experimental Section

Materials. A Ru/Al_2O_3 catalyst (Ru loading, 0.5 wt %) was obtained from Nippon Engelhardt Ltd. Before use, it was ground into a fine powder and reduced in flowing H_2 at 723 K for 3 h. The number of surface Ru atoms was determined by a conven-

(1) Tamaru, K. "Dynamic Heterogeneous Catalysis"; Academic Press: New York, 1978.

(2) (a) Kobayashi, H.; Kobayashi, M. *Catal. Rev.* **1974**, *10*, 139. (b) Bennett, C. O. *Ibid.* **1976**, *13*, 121. (c) Matsumoto, H.; Bennett, C. O. *J. Catal.* **1978**, *53*, 331. (d) Reymond, J. P.; Mériaudeau, P.; Pommier, B.; Bennett, C. O. *Ibid.* **1980**, *64*, 163. (e) Cant, N. W.; Bell, A. T. *Ibid.* **1982**, *73*, 257.

(3) (a) Murakami, Y. "Some Theoretical Problems of Catalysis"; Kwan, T., Boreskov, G. K., Tamaru, K. Eds.; University of Tokyo Press: Tokyo, 1973; p 203. (b) Hattori, T.; Shirai, K.; Niwa, M.; Murakami, Y. *React. Kinet. Catal. Lett.* **1980**, *15*, 193.

(4) Hattori, T.; Murakami, Y. *Can. J. Chem. Eng.* **1974**, *52*, 601.

(5) Hattori, T.; Kanetake, K.; Murakami, Y. *Nippon Kagaku Kaishi* **1977**, 1957.

(6) (a) Mori, T.; Masuda, H.; Imai, H.; Murakami, Y. *Nippon Kagaku Kaishi* **1979**, 1449. (b) Mori, T.; Masuda, H.; Imai, H.; Miyamoto, A.; Baba, S.; Murakami, Y. *J. Phys. Chem.* **1982**, *86*, 2753. (c) Mori, T.; Masuda, H.; Imai, H.; Miyamoto, A.; Hasebe, R.; Murakami, Y. *Ibid.* **1983**, *87*, 3648. (d) Niizuma, H.; Hattori, T.; Mori, T.; Miyamoto, A.; Murakami, Y. *Ibid.* **1983**, *87*, 3652.

(7) (a) Vannice, M. A. *Catal. Rev.* **1976**, *14*, 153. (b) Ponec, V. *Ibid.* **1978**, *18*, 151. (c) Denny, P. J.; Whan, D. A. *Catalysis (London)* **1978**, *2*, 46. (d) Bell, A. T. *Catal. Rev.* **1981**, *23*, 203. (e) Biloen, P.; Sachtler, W. M. H. *Adv. Catal.* **1981**, *30*, 165. (f) Vannice, M. A. "Catalysis—Science and Technology"; Springer-Verlag: West Berlin, 1982; Vol. 3, Chapter 3. (b) Ponec, V. *Catalysis (London)* **1982**, *5*, 48. (h) Kelley, R. D.; Goodman, D. W. "The Chemical Physics of Solid Surfaces and Heterogeneous Catalysis"; Elsevier: Amsterdam, 1982; Chapter 10 and references therein.

0022-3654/86/2090-0109$01.50/0

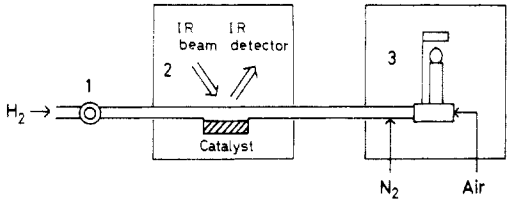

Figure 1. Construction of the PSRA–EDR–FID apparatus: 1, inlet of the reactant pulse; 2, emissionless infrared diffuse reflectance spectrometer (EDR); 3, flame ionization detector (FID).

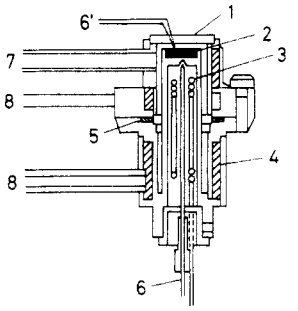

Figure 2. Details of the EDR cell: 1, KBr window; 2, catalyst; 3, heater; 4, cooling water; 5, O-ring or aluminum gasket; 6 and 6', thermocouple; 7, pipe for flowing gas; 8, pipe for cooling water.

tional pulse method of CO adsorption to be 14.5 μmol (g of catalyst)$^{-1}$. Commerical CO, CH_4, and N_2 were used without further purification. H_2 was purified by passing it through a Pd/Al_2O_3 catalyst at room temperature in order to remove O_2 as a possible impurity.

Apparatus and Procedure. As shown in Figure 1, the new PSRA apparatus (PSRA–EDR–FID) was composed of the following parts: inlet of reactant pulse (1), Jasco EDR-31 emissionless infrared diffuse reflectance spectrometer (EDR) (2), and flame ionization detector (FID) (3). The connections between the inlet of the reactant pulse, EDR, and FID were made with 3-mm tubings and fittings. The basic optical unit for the EDR was described elsewhere.[8] Figure 2 shows the details of the EDR cell. The catalyst powder (2 in Figure 2) was packed just under the KBr window (1) and heated by the underlying heater (3). The carrier gas (H_2) flows from the inlet pipe (7) to the outlet pipe (behind 7) through the catalyst bed (2). The cell volume was approximately 1 cm^3. The observation of the reaction temperature was made with a thermocouple (6') located just at the top of the catalyst bed.

A prereduced Ru/Al_2O_3 powder was packed in the EDR cell and subjected to in situ reduction with a stream of H_2 at 573 K for 1 h. A small amount of CO (usually 10 μL (STP)) was injected from the pulse inlet (1 in Figure 1) into flowing H_2 gas (flow rate, 50 cm^3 (STP) min^{-1}). It was adsorbed on the catalyst, and the adsorbed CO was hydrogenated with H_2 to form CH_4 and H_2O; the methanation took place selectively under the conditions of the PSRA experiments. The dynamics of the adsorbed species was measured by the EDR (2 in Figure 1) while that of the gaseous product (CH_4) was detected by the FID (3). The conventional PSRA apparatus (PSRA–FID) was the same as those used in the previous investigations.[3-6]

A small amount of CO (usually 10 μL (STP)) was injected from the pulse inlet (1 in Figure 1) into flowing H_2 gas (flow rate, 50 cm^3 (STP) min^{-1}).[16]

Results

Dynamics of Nonreacting Species. Before investigating the dynamics of surface reactions, we examined the dynamics of nonreacting species. When a CO pulse (10 μL (STP); the width at half-height was 2 s) was introduced in the presence of Al_2O_3 (or KBr) instead of the Ru/Al_2O_3 catalyst, IR absorption bands of the gaseous CO appeared and then disappeared within 5 s. When various amounts of CO pulses were introduced to the Ru/Al_2O_3 catalyst at 326 K, an IR absorption band was observed at around 2040 cm^{-1}, which is assignable to a linearly adsorbed

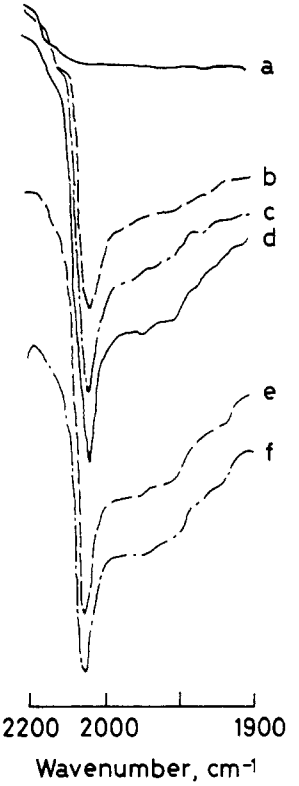

Figure 3. Infrared spectra of CO adsorbed on Ru/Al_2O_3 catalyst at 326 K for various amounts of the CO pulse: a, background; b, 5 μL (STP); c, 10 μL (STP); d, 100 μL (STP); e, 200 μL (STP); f, 1 mL (STP).

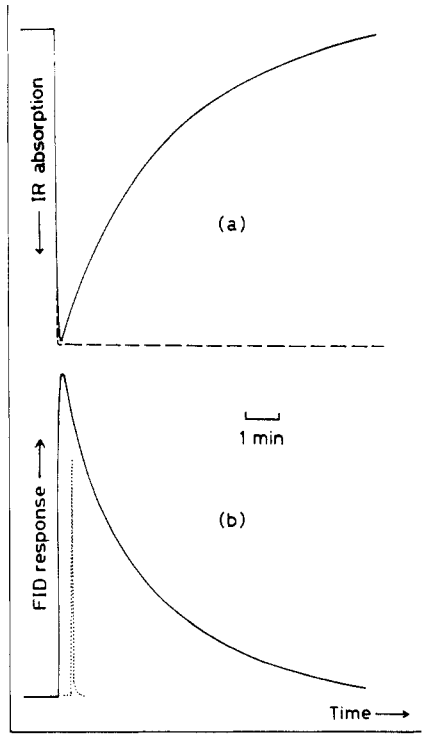

Figure 4. Dynamic behaviors of adsorbed CO (a) and produced CH_4 (b) after the introduction of the CO pulse to the Ru/Al_2O_3 catalyst at 411 K (H_2 flow rate, 50 cm^3 min^{-1}; amount of the CO pulse, 10 μL (STP)). The broken line in (a) is the EDR response after the CO pulse at 326 K, and the sharp dotted line in (b) is the FID response of CH_4 pulsed at 411 K instead of CO.

(8) (a) Niwa, M.; Hattori, T.; Takahashi, M.; Shirai, K.; Watanabe, M.; Murakami, Y. *Anal. Chem.* **1979**, *51*, 46. (b) Hattori, T.; Shirai, K.; Niwa, M.; Murakami, Y. *Ibid.* **1981**, *53*, 46. (c) Hattori, T.; Shirai, K.; Niwa, M.; Murakami, Y. *Bull. Chem. Soc. Jpn.* **1981**, *54*, 1964.

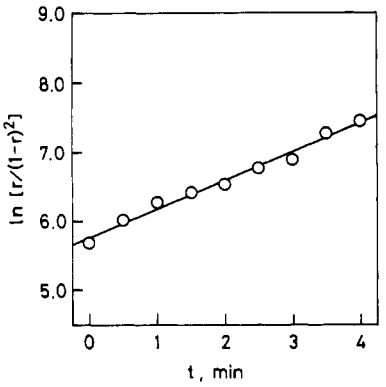

Figure 5. Relationship between $\ln [r/(1-r)^2]$ and t at 411 K.

CO on the Ru metal (Figure 3).[9] Although the band position of the linear CO shifted to the higher frequency with an increasing amount of the CO pulse, it was almost constant (at 2040 cm^{-1}) for the amount of the CO pulse less than 10 μL (STP). Figure 4a shows the change in the intensity of the 2040-cm^{-1} band with time after the CO pulse (dashed line in Figure 4a). As shown, the adsorption of CO immediately took place (within 5 s) and the linear CO was stably adsorbed on the Ru/Al_2O_3 catalyst; the reaction of adsorbed CO to CH_4 was negligible, when the catalyst temperature was as low as 326 K.

Dynamics of Adsorbed CO and Produced CH_4 under Methanation. When the CO pulse was introduced to the Ru/Al_2O_3 catalyst at elevated temperatures, the IR absorption band of linear CO also appeared at 2040 cm^{-1} but its intensity gradually decreased with time. Figure 4a shows the EDR response at 2040 cm^{-1} after the CO pulse at 411 K (solid line). Figure 4b shows the dynamics of CH_4 produced from the CO pulse. As shown, the FID response for the produced CH_4 immediately increased after the CO pulse and then gradually decreased with time. As shown by the dotted line in Figure 4b, when CH_4 was pulsed instead of CO, it was immediately eluted from the catalyst (the width at half-height was less than 5 s). Since desorption of CO was negligible under the present experimental conditions, these results indicate that the linear CO gradually reacts with H_2 to produce CH_4 and H_2O. The dynamics of the linear CO and CH_4 were similarly measured under various conditions.

Rate Constants of Surface Reactions. It is well accepted that, in the CO hydrogenation, CH_4 is produced through the hydrogenation of surface carbon species $[(CH_x)_{ad}]$ formed from the dissociation of the C–O bond of adsorbed CO $[(CO)_{ad}]$. This can be shown by the following consecutive reaction, although each step is also composed of several steps

$$(CO)_{ad} \xrightarrow{k_{CO}} (CH_x)_{ad} \xrightarrow{k_{CH_x}} CH_4 \qquad (1)$$

where k_{CO} and k_{CH_x} are the rate constants for the reaction $(CO)_{ad} \rightarrow (CH_x)_{ad}$ and $(CH_x)_{ad} \rightarrow CH_4$, respectively. If the reaction $(CO)_{ad} \rightarrow (CH_x)_{ad}$ is first order with respect to the amount of $(CO)_{ad}$, the reaction rate is

$$-(dN_{CO})/dt = k_{CO}N_{CO} \qquad (2)$$

where N_{CO} is the amount of the linearly adsorbed CO. According to the Kubelka–Munk equation,[10] N_{CO} is given by

$$\alpha N_{CO} = (1-r)^2/2r \qquad (3)$$

where r is the relative reflectance at 2040 cm^{-1} and α is a proportionality constant. Integration of eq 2 leads to

$$\ln [r/(1-r)^2] = k_{CO}t + \ln [r_0/(1-r_0)^2] \qquad (4)$$

where r_0 is r at $t = 0$. Equation 4 indicates that the rate constant k_{CO} can be determined from the slope of the linear relationship between $\ln [r/(1-r)^2]$ and t. Figure 5 shows an example of the experimental relationships between $\ln [r/(1-r)^2]$ and t. As shown, a straight line was obtained, which assures the assumption of the first-order reaction. From the slope of the linear relationship, k_{CO} was determined and the results of k_{CO} under various conditions are shown in Figure 6 as a function of the reaction temperature (T). As shown, k_{CO} satisfies the Arrhenius equation; the activation energy and preexponential factor are 72.4 kJ mol^{-1} and 1.4×10^7 s^{-1}, respectively.

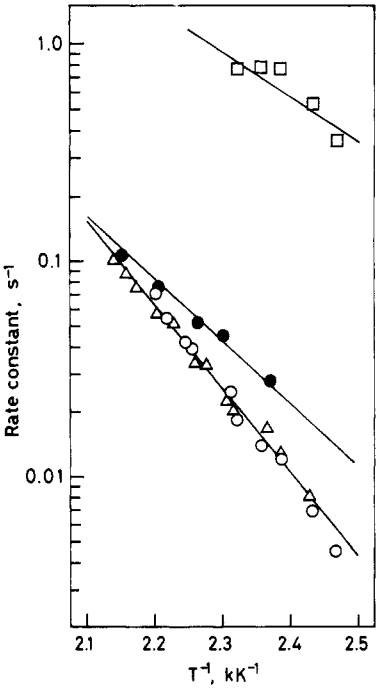

Figure 6. Arrhenius plots of the rate constants of k_{CO} (○) and k_{CH_x} (□). △ and ● are the rate constants determined by the PSRA–FID apparatus from the dynamics of produced CH_4 in flowing H_2 (k_{CO}^H) and D_2 (k_{CO}^D), respectively.

As shown in Figure 3, the IR absorption band has a shoulder peak at around 1950 cm^{-1}, which may be assignable to bridge CO. The reactivity of the bridge CO with H_2 was also investigated by measuring the dynamics of this band. It was found that the bridge CO was much less reactive than the linear CO at any temperatures examined.

The formation rates of $(CH_x)_{ad}$ and CH_4 are given by eq 5 and 6, respectively

$$dN_{CH_x}/dt = k_{CO}N_{CO} - k_{CH_x}N_{CH_x} \qquad (5)$$

$$dN_{CH_4}/dt = k_{CH_x}N_{CH_x} \qquad (6)$$

where N_{CH_x} and N_{CH_4} are the amounts of $(CH_x)_{ad}$ and CH_4, respectively. These equations are solved to give the following equation

$$v(t) = \frac{dN_{CH_4}}{dt} = \frac{k_{CO}k_{CH_x}N^\circ_{CO}}{k_{CH_x} - k_{CO}}[\exp(-k_{CO}t) - \exp(-k_{CH_x}t)] \qquad (7)$$

where $v(t)$ is the rate of CH_4 formation and N°_{CO} is N_{CO} at $t = 0$. The value of k_{CH_x} was determined by a least-squares fit of the decay curve of CH_4 with eq 7.[11] Figure 7 shows an example of the results; k_{CH_x} was determined to be 0.531 s^{-1} for the result. The results of k_{CH_x} under various conditions were similarly determined, and the results are also shown in Figure 6.

If k_{CH_x} is much larger than k_{CO}, then eq 7 can be approximated by

$$v(t) = k_{CO}N^\circ_{CO} \exp(-k_{CO}t) \qquad (8)$$

$$\ln v(t) = \ln k_{CO}N^\circ_{CO} - k_{CO}t \qquad (9)$$

(9) (a) Brown, M. F.; Gonzalez, R. D. *J. Phys. Chem.* **1976**, *80*, 1731. (b) Ekerdt, J. G.; Bell, A. T. *J. Catal.* **1979**, *58*, 170. (c) Yamazaki, H.; Kobori, Y.; Naito, S.; Onishi, T.; Tamaru, K. *J. Chem. Soc., Faraday Trans. 1* **1981**, *77*, 2913.

(10) Kubelka, P.; Munk, F. *Z. Tech. Phys.* **1931**, *12*, 593.

(11) Under the constant flow rate of the carrier gas, $v(t)$ is proportional to the FID response in the decay curve of produced CH_4.

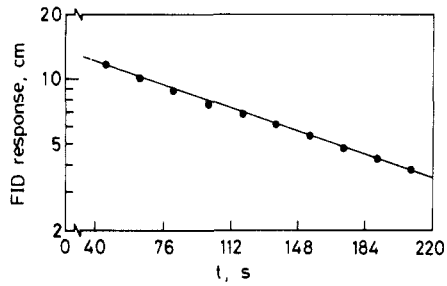

Figure 7. Relationship between FID response and t at 411 K. The solid line shows the values calculated from eq 7. Although $v(t)$ is proportional to the FID response under the constant flow rate of the carrier gas, the proportionality constant is not known. The calculation was, therefore, carried out so that the first point of the experimental value agreed with the calculated one.

Equation 9 indicates that ln (FID response) vs. t gives the straight line, and k_{CO} is determined from its slope. In other words, the rate constant k_{CO} can be directly determined from the decay curve of produced CH_4 in the case of $k_{CH_x} >> k_{CO}$. The values of k_{CO} thus determined are also shown in Figure 6. As shown, both methods give the same values of k_{CO} at any temperature examined.

The rate constant in flowing D_2 was also determined by the PSRA–FID, and the results are shown in Figure 6. As shown, the rate constant is larger in D_2 than in H_2, indicating the inverse isotope effect on k_{CO}. The average value of the isotope effect (k^H_{CO}/k^D_{CO}) was 0.78.

Discussion

Availability of the PSRA–EDR–FID. Although the results shown in Figures 5–7 indicate the availability of the proposed method, the following points should be noted as further evidence for its validity. For the measurement of the dynamics of adsorbed species and product molecule, it is necessary that pulses of the reactant and the product do not disperse in the tubings from the inlet to the catalyst bed and from the catalyst bed to the FID and that the mass transfer of the reactant from the gas stream to the catalyst surface is sufficiently rapid compared with the surface reaction. In order to satisfy the former criterion, the present apparatus was designed to decrease the dead volume from the inlet of the reactant pulse to the FID: The volume of the EDR cell (ca. 1 cm^3) is much smaller than that of the conventional infrared cell for surface measurements. The inside diameter of the tubings was as small as 2 mm. By the improvement, the dispersion of the reactant pulse from the inlet to the catalyst bed and that of the product from the catalyst bed to the FID was decreased. As shown for the example in Figure 4, the dispersion was within 5 s. The latter criterion—rapid mass transfer—is considered to be satisfied from the results of the EDR response of linear CO. As shown in Figure 4a, the adsorption of CO was completed within 5 s after the CO pulse. Since the time scale of decay in the present experiments was much larger than 5 s, the effect of dispersion is negligible in the rate constants.

Rate Constants and Rate-Determining Step. As shown in Figure 6, k_{CH_x} is much larger than k_{CO}, indicating that the dissociation of $(CO)_{ad}$ to $(CH_x)_{ad}$ and $(OH_y)_{ad}$ mainly determines the rate of CH_4 formation from $(CO)_{ad}$. This is consistent with the results in Figure 6 that k_{CO} determined from the dynamics of $(CO)_{ad}$ is almost equal to k_{CO} determined from eq 8 or 9 under the assumption $k_{CH_x} >> k_{CO}$. The large value of k_{CH_x} relative to k_{CO} means that the formation of $(CH_x)_{ad}$ is much slower than its hydrogenation and therefore that the concentration of $(CH_x)_{ad}$ is much lower than that of $(CO)_{ad}$. This is consistent with the experimental result that no noticeable band appears at the C–H stretching region in the EDR–IR spectra under the steady-state CO hydrogenation on Ru/Al_2O_3.[12] We have previously found that CH_4 and H_2O are produced with almost equal rates in the hydrogenation of a CO pulse in flowing H_2.[13] Since the hydrogenation of $(OH_y)_{ad}$ to H_2O is considered to proceed readily, this is in accordance with the relationship $k_{CO} << k_{CH_x}$.

TABLE I: Observed Preexponential Factor (A) and Isotope Effect (k^H_{CO}/k^D_{CO}) for the Supported Metal Catalysts

metal	A, s^{-1}	k^H_{CO}/k^D_{CO}
Fe[a]	3.9×10^9	0.82
Ni[b]	5.4×10^6	0.75
Ru	1.4×10^7	0.78
Pd[c]	1.6×10^4	0.61

[a] Reference 17. [b] Reference 6b. [c] Reference 6c.

TABLE II: Variation of the Preexponential Factor (A) and Isotope Effect (k^H_{CO}/k^D_{CO}) with the Number of Hydrogen Atoms Involved in the Intermediate (n)[6b,c]

n	A, s^{-1}	k^H_{CO}/k^D_{CO}
0	10^{13}	1.0
1	10^{10}	0.85
2	10^7	0.74
3	10^4	0.56

Mechanism of the C–O Bond Dissociation. As described above, the rate constant for the C–O bond dissociation (k_{CO}), the Arrhenius parameters, and the H_2–D_2 isotope effect (k^H_{CO}/k^D_{CO}) were determined for the methanation on Ru/Al_2O_3. It is interesting to note that an H_2–D_2 inverse isotope effect was observed for k_{CO} (0.78). Furthermore, the preexponential factor of k_{CO} (1.4×10^7 s^{-1}) is much smaller than that for a simple unimolecular decomposition of adsorbed CO molecule to surface carbon $[(C)_{ad}]$ and oxygen $[(O)_{ad}]$ atoms (ca. 10^{13} s^{-1}).[6b,c] These results suggest that the dissociation of the C–O bond in the CO hydrogenation is not a simple one of $(CO)_{ad}$ to $(C)_{ad}$ and $(O)_{ad}$ and that hydrogen atoms play an important role in the C–O bond dissociation process. This is in accordance with the conclusion obtained by Cant and Bell by using the transient method.[2e]

Rate Parameters for the C–O Bond Dissociation on Various Metals. Since the dissociation of the C–O bond is the rate-determining step for the methanation on Ni/SiO_2, Pd/Al_2O_3, and Fe/Al_2O_3 catalysts under the PSRA condition,[6,13] the Arrhenius parameters and H_2–D_2 isotope effect for k_{CO} have been determined by the previous PSRA–FID apparatus. As shown in Table I,[6b,c,17] the H_2–D_2 inverse isotope effect is observed for all catalysts. Furthermore, the preexponential factor of k_{CO} is considerably smaller than that for the unimolecular decomposition of $(CO)_{ad}$ (ca. 10^{13} s^{-1}) for all catalysts. It should be noted however that the magnitude of the inverse isotope effect or preexponential factor changes with the type of catalyst. The order of the inverse isotope effect is Fe < Ni = Ru < Pd, and that of the preexponential factor is Fe > Ni = Ru > Pd.

In order to explain the inverse isotope effect and the magnitude of the preexponential factor for k_{CO}, we have previously proposed the following mechanism of the C–O bond dissociation:[6]

$$(CO)_{ad} \rightleftarrows (COH_n)_{ad} \not\rightarrow (CH_x)_{ad} + (OH_y)_{ad} \qquad (10)$$

Taking into account recent knowledge in organometallic chemistry, a partially hydrogenated CO species $[(COH_n)_{ad}]$—such as formyl, hydroxycarbene, and hydroxymethyl species—is considered in this mechanism as an intermediate of the C–O bond dissociation,[14] of which process is found to be the rate-determining step as shown in the preceding discussion. Table II shows the results of the inverse isotope effect and preexponential factor calculated by using the transition-state theory.[6b,c] As shown, the magnitude of H_2–D_2 inverse isotope effect or the preexponential factor changes with the number of hydrogen atoms (n) in $(COH_n)_{ad}$. From the comparison of the calculated result (Table II with the experimental one (Table I), the difference in the rate parameters among metals may be brought about by the difference in n: 1 for Fe, 2 for Ni and Ru, and 3 for Pd.

(12) Mori, T.; Miyamoto, A.; Takahashi, N.; Fukagaya, M.; Hattori, T.; Murakami, Y., to be submitted for publication.

(13) Mori, T.; Masuda, H.; Imai, H.; Miyamoto, A.; Murakami, Y. *Nippon Kagaku Kaishi* **1982**, 162.

(14) Costa, L. C. *Catal. Rev.* **1983**, *25*, 325 and references therein.

Recent studies about catalyst surfaces by means of electron spectroscopy or the TPD (temperature-programmed desorption) method have revealed that adsorbed CO is readily dissociated on metals in the absence of H_2; its dissociation takes place at room temperature for Fe, at around 400 K for Ni and Ru, and above 573 K for Pd.[15] The order of ability of C–O bond dissociation in the absence of H_2 (Fe > Ni = Ru > Pd) is correlated to that of the inverse isotope effect or preexponential factor for k_{CO} in the presence of H_2 and therefore to the number of hydrogen atoms in $(COH_n)_{ad}$ (Fe < Ni = Ru < Pd). The n in $(COH_n)_{ad}$ is small on a metal with high activity for the C–O bond dissociation in the absence of H_2 (Fe), while it is large for a metal with low activity for the C–O bond dissociation (Pd). This is reasonable since the effect of hydrogen seems more important on a metal with less activity for the C–O bond dissociation.

(15) (a) Joyner, R. W.; Roberts, M. W. *J. Chem. Soc., Faraday Trans. 1* **1974**, *70*, 1819. (b) Kishi, K.; Roberts, M. W. *Ibid.* **1975**, *71*, 1715. (c) Broden, G.; Rhodin, T. N.; Brucker, C.; Benbow, R.; Hurych, Z. *Surf. Sci.* **1976**, *59*, 593. (d) Broden, G.; Gafner, G.; Bonzel, H. P. *Appl. Phys.* **1977**, *13*, 333. (e) Rhodin, T. N.; Brucker, C. F. *Solid State Commun.* **1977**, *23*, 275. (f) Rabo, J. A.; Risch, A. P.; Poutsma, M. L. *J. Catal.* **1978**, *53*, 295. (g) Erley, W.; Wagner, H. *Surf. Sci.* **1978**, *74*, 333. (h) Bertolini, J. C.; Imelik, B. *Ibid.* **1979**, *80*, 586. (i) Erley, W.; Ibach, H.; Lehwald, S.; Wagner, H. *Ibid.* **1979**, *83*, 585. (j) McCarty, J. G.; Wise, H. *Chem. Phys. Lett.* **1979**, *61*, 323. (k) Low, G. G.; Bell, A. T. *J. Catal.* **1979**, *57*, 397. (l) Galuszka, J.; Chang, J. R.; Amenomiya, Y. *Ibid.* **1981**, *68*, 172.

(16) This assures as discussed later that the band position is constant in the IR absorption spectra and also that the rate constant can be determined without any effect from the fractional surface coverage of H_2.

(17) Masuda, H.; Imai, H.; Mori, T. *Rep. Gov. Ind. Res. Inst., Nagoya* **1985**, *34*, 113.

Conclusions

In the present study, we have developed a new PSRA apparatus (PSRA–EDR–FID) which enables us the simultaneous measurements of the dynamics of both adsorbed species and product molecules. It has also been proved that the rate constants of surface reactions can be determined from their dynamics. It should, however, be noted that the present EDR is not sensitive enough to observe the dynamics of various adsorbed species, and only the dynamics of adsorbed CO was measured in this study. Many instruments have recently been developed to sensitively detect adsorbed species. The combination of PSRA with these instruments would lead to the determination of rate constants of various steps. The present paper describes an example of a way to determine the rate constants from the dynamics of adsorbed species and product molecules.

Acknowledgment. We gratefully acknowledge the invaluable assistance by Mr. T. Kaminishi for computer calculations. This work was partially supported by a Grant-in-Aid for Energy Research from the Ministry of Education, Science and Culture, Japan (No. 59040015).

Registry No. CO, 630-08-0; Ru, 7440-18-8.

An Anomalous Phase Effect in the Individual Hyperfine Lines of the CIDEP Spectra Observed in the Photochemical Reactions of Benzophenone in Micelles

Hisao Murai,† Yoshio Sakaguchi, Hisaharu Hayashi,*

The Institute of Physical and Chemical Research, Wako, Saitama 351-01, Japan

and Yasumasa J. I'Haya

Department of Materials Science and Laboratory of Magneto-Electron Physics, The University of Electro-Communications, Chofu, Tokyo 182, Japan *(Received: August 6, 1985)*

Photochemical reactions in some micellar solutions of benzophenone and its derivatives are studied by CIDEP. Each of the CIDEP spectra observed immediately (1.2 μs) after laser excitation of the solutions was found to consist of the corresponding ketyl radical and the alkyl radical produced from a micellar molecule. An alternating-phase pattern was observed in each of the hf lines of the alkyl radicals. Later, this anomalous phase pattern gradually changed to the ordinary E/A pattern of the radical pair mechanism. Some origins of this phenomenon are discussed and intramolecular hydrogen migration of the alkyl radical is proposed as the most probable model for this phenomenon.

Introduction

Magnetic field effects on photochemical reactions in solution have been extensively studied during the past decade.[1] Among other things, large magnetic field effects on the reaction rates and yields of intermediate radicals in micelles have been observed.[1] The magnetic field effects observed in usual solvents are known to be classified and systematically interpreted in terms of the Δg, hyperfine coupling (hfc), and level-crossing mechanisms.[2] However, these mechanisms could not explain the large magnetic field effects observed in micelles.[3]

A recent proposal of the relaxation mechanism (RM) for the magnetic field effects in micelles made by Hayashi and Nagakura seems to be most appropriate;[4] the relaxation of the electron spins in a radical pair plays an important role. However, most of the data concerning the magnetic field effects reported so far have been measured by product analysis and/or by time-resolved absorption spectroscopy in the visible and ultraviolet region. On the other hand, chemically induced dynamic electron polarization (CIDEP) is expected to give direct information about the formation and decay of the electron polarization of the intermediate radical pairs.[5]

Recently, we have carried out CIDEP studies of the photoreduction of naphthoquinone, benzophenone, and xanthone in sodium

† On leave from The University of Electro-Communications.

(1) Y. Sakaguchi and H. Hayashi, *J. Phys. Chem.*, **88**, 1437 (1984), and references cited therein.

(2) H. Hayashi and S. Nagakura, *Bull. Chem. Soc. Jpn.*, **51**, 2862 (1978); Y. Sakaguchi, H. Hayashi, and S. Nagakura, *ibid.*, **53**, 39 (1980).

(3) Y. Sakaguchi, S. Nagakura, and H. Hayashi, *Chem. Phys. Lett.*, **72**, 420 (1980); Y. Sakaguchi and H. Hayashi, *ibid.*, **87**, 539 (1982).

(4) H. Hayashi and S. Nagakura, *Bull. Chem. Soc. Jpn.*, **57**, 322 (1984).

(5) J. K. S. Wan, *Adv. Photochem.*, **12**, 283–346 (1980); C. D. Buckley and K. A. McLaughlan, *Mol. Phys.*, **54**, 1 (1985), and references cited therein.

0022-3654/86/2090-0113$01.50/0